

# Exotic $T_{c\bar{s}0}^a(2900)^0$ and $T_{c\bar{s}0}^a(2900)^{++}$ States in Born-Oppenheimer Approximation

Halil Mutuk<sup>1,\*</sup>

<sup>1</sup>*Department of Physics, Faculty of Science, Ondokuz Mayıs University, 55200, Samsun, Türkiye*  
(Dated: December 2, 2025)

We employ Born-Oppenheimer approximation to the  $T_{c\bar{s}0}^a(2900)^0$  and  $T_{c\bar{s}0}^a(2900)^{++}$  states observed by the LHCb Collaboration and study mass spectrum and root-mean-square radius values. For this purpose, we use dynamical diquark model. We assume that strange quark is a heavy for the usage of Born-Oppenheimer approximation. Our results strongly indicate that the  $T_{c\bar{s}0}^a(2900)$  states are best described as composed of axial-vector (spin-1) diquark pairs. Furthermore, the calculated root-mean-square radius,  $\langle r^2 \rangle^{1/2} \approx 0.70 - 0.80$  fm, which is significantly less than 1 fm, provides compelling evidence that these are compact tetraquarks rather than loosely bound hadronic molecules.

Keywords: exotic hadrons, open-flavor tetraquarks, Born-Oppenheimer approximation, diquark

## I. INTRODUCTION

In 1964, Murray Gell-Mann [1] and George Zweig [2] independently proposed a classification scheme for hadrons in terms of valence quarks and antiquarks. This scheme, so-called quark model, classifies hadrons into two groups: mesons which are quark-antiquark bound states and baryons which are three-quark bound states. The quark model explained properties of the observed hadron spectrum quite well upto 2000s. This paradigm turned into a different path when the Belle Collaboration announced observation of X(3872) particle in the charmonium energy region [3]. This particle decays to  $J/\psi \rightarrow \pi^+\pi^-$  and  $J/\psi \rightarrow \pi^+\pi^-\pi^0$  and cannot be a pure charmonium  $c\bar{c}$  state. This was the first exotic hadron that do not fall into the quark model predictions. Actually, QCD, the theory of strong interactions, allows the existence of more complex structures (multi-quark states), so-called exotic hadrons. These exotic states include tetraquarks, pentaquarks, hexaquarks, hybrids, and glueballs. Perpetual efforts on experiments revealed the existence of some of them (four-quark states and pentaquarks for the time being).

In 2020, the LHCb Collaboration carried out amplitude analyses of the decays  $B^+ \rightarrow D^+D^-K^+$  [4, 5] resulting two new resonant states. The Breit-Wigner mass and width of the new resonant states are

$$T_{cs0}(2900)^0 : M = (2866 \pm 7 \pm 2) \text{ MeV}, \quad \Gamma = (57 \pm 12 \pm 4) \text{ MeV}, \quad (1)$$

$$T_{cs1}(2900)^0 : M = (2904 \pm 5 \pm 1) \text{ MeV}, \quad \Gamma = (110 \pm 11 \pm 4) \text{ MeV}. \quad (2)$$

where the first uncertainties are statistical and the second systematic. The quantum numbers of these states are  $J^P = 0^+$  for  $T_{cs0}(2900)^0$  and  $J^P = 1^-$  for  $T_{cs1}(2900)^0$  with minimal quark flavor content  $ud\bar{c}\bar{s}$ .

In December 2022, the LHCb collaboration reported two new states  $T_{c\bar{s}0}^a(2900)^0$  and  $T_{c\bar{s}0}^a(2900)^{++}$  in the  $D_s^+\pi^-$  and  $D_s^+\pi^+$  invariant mass distributions of the processes  $B^0 \rightarrow \bar{D}^0 D_s^+ \pi^-$  and  $B^+ \rightarrow D^- D_s^+ \pi^+$  decays, respectively [6, 7]. The statistical significance is found to be  $8\sigma$  for the  $T_{c\bar{s}0}^a(2900)^0$  and  $6.5\sigma$  for the  $T_{c\bar{s}0}^a(2900)^{++}$  state. The Breit-Wigner mass and width of these states are

$$T_{c\bar{s}0}^a(2900)^0 : M = (2892 \pm 14 \pm 15) \text{ MeV}, \quad \Gamma = (119 \pm 26 \pm 13) \text{ MeV}, \quad (3)$$

$$T_{c\bar{s}0}^a(2900)^{++} : M = (2921 \pm 17 \pm 20) \text{ MeV}, \quad \Gamma = (137 \pm 32 \pm 17) \text{ MeV}. \quad (4)$$

These two states should be part of the same isospin triplet because of their similar masses and widths. Indeed, the quantum numbers of both states are determined to be  $I(J^P) = 1(0)^+$ . The minimal quark flavor components may be  $\bar{c}\bar{s}ud$  for  $T_{c\bar{s}0}^a(2900)^0$  state and  $c\bar{s}u\bar{d}$  for  $T_{c\bar{s}0}^a(2900)^{++}$  state. The  $T_{c\bar{s}0}^a(2900)$  is located near the  $D^*K^*$  threshold. Therefore, according to certain studies it appears as  $D^*K^*$  hadronic molecule [8–10]. Besides that compact tetraquark picture is also applied in Refs. [11–15]. Ref. [16] indicates the presence of a binding mechanism in the isovector  $D^*K^*$  system. In Ref. [17],  $T_{c\bar{s}0}^a(2900)^0$  and  $T_{c\bar{s}0}^a(2900)^{++}$  states are modelled as  $D_s^{*+}\rho^+$  and  $D_s^{*+}\rho^-$  molecules by using two-point QCD sum rule method. In a coupled-channel approach [18], it is observed that  $T_{c\bar{s}0}(2900)$  can also be considered as a virtual state created by the  $D_s^*\rho$  and  $D^*K^*$  interactions. Using the same approach,  $T_{c\bar{s}0}(2900)$

\* [hmutuk@omu.edu.tr](mailto:hmutuk@omu.edu.tr)

were found to be as a bound/virtual state in  $D^*K^*-D_s^*\rho$  coupled-channel interactions [19]. It is suggested in Ref. [20] to search  $T_{c\bar{s}0}^a(2900)^{++}$  also in the  $B^+ \rightarrow K^+D^+D^-$  process. In Ref. [21], an effective potential model is used to study  $\bar{D}^*K^*$  and  $D^{(*)}K^*$  systems. They predict many states in these systems indicating that  $T_{cs0}(2900)$  and  $T_{c\bar{s}0}^a(2900)$  states can be well identified as the  $I(J^P) = 0(0^+)$  and  $I(J^P) = 1(0^+)$  partners of  $T_{cc}$  and  $Z_c$  in the charmed-strange sector, respectively. In the invariant mass distribution of  $D_s^- \pi^+$ ,  $T_{c\bar{s}0}(2900)$  is expected to be detected at around 2900 MeV [22]. Ref. [23] studied  $T_{cs0}$  and  $T_{c\bar{s}0}$  states via using the diffusion Monte Carlo (DMC) method within the framework of the constituent quark model. They describe these states as compact structures, neither diquark/antidiquark nor meson/meson pictures. The results indicate that observed resonances are in both cases excited flavor states with  $I = 1$ . Ref. [24] investigated the production of the  $T_{c\bar{s}1}^0$  state, interpreted as an  $S$ -wave  $\bar{D}K^*$  hadronic molecule with  $I(J^P) = 0(1^+)$ , in  $B^+$  meson decays. Using an effective Lagrangian approach and meson loop mechanisms, the authors predict branching ratios of the order  $10^{-5}$ – $10^{-4}$  for  $B^+ \rightarrow D^{(*)+}T_{c\bar{s}1}^0$  and suggest searching for this state in the  $B^+ \rightarrow D^{*+}D^{*-}K^+$  channel at Belle II and LHCb.

In 2024, a study of resonant structures in  $B^+ \rightarrow D^{*+}D^-K^+$  and  $B^+ \rightarrow D^{*-}D^+K^+$  decays is performed, using proton-proton collision data at centre-of-mass energies of  $\sqrt{s} = 7, 8$ , and 13 TeV by the LHCb Collaboration [25]. In addition to charmonium-like states  $\eta_c(3945)$ ,  $h_c(4000)$ ,  $\chi_{c1}(4010)$  and  $h_c(4300)$ , the existence of the  $T_{c\bar{s}0}^*(2870)^0$  and  $T_{c\bar{s}1}^*(2900)^0$  resonances in the  $D^-K^+$  mass spectrum, already observed in the  $B^+ \rightarrow D^+D^-K^+$  decay, is confirmed in a different production channel with corresponding masses and width values:

$$T_{c\bar{s}0}^*(2870)^0 : \quad M = (2914 \pm 11 \pm 15) \text{ MeV}, \quad \Gamma = (128 \pm 22 \pm 23) \text{ MeV}, \quad (5)$$

$$T_{c\bar{s}1}^*(2900)^0 : \quad M = (2887 \pm 8 \pm 6) \text{ MeV}, \quad \Gamma = (92 \pm 16 \pm 16) \text{ MeV}. \quad (6)$$

A comparison of mass and width values of previous and present experiments is given in Table I.

TABLE I. Comparison of the  $T_{c\bar{s}0,1}^*$  properties obtained in Ref. [25] to those found previously in  $B^+ \rightarrow D^+D^-K^+$  decays Ref. [4].

Physical Properties	Present Exp.[25]	Previous Exp. [4]
$T_{c\bar{s}0}^*(2870)^0$ mass [MeV]	$2914 \pm 11 \pm 15$	$2866 \pm 7$
$T_{c\bar{s}0}^*(2870)^0$ width [MeV]	$128 \pm 22 \pm 23$	$57 \pm 13$
$T_{c\bar{s}1}^*(2900)^0$ mass [MeV]	$2887 \pm 8 \pm 6$	$2904 \pm 5$
$T_{c\bar{s}1}^*(2900)^0$ width [MeV]	$92 \pm 16 \pm 16$	$110 \pm 12$

Motivated by this latest experimental observation, in this work, we apply the dynamical diquark model to explore the spectrum of charm–strange tetraquarks, often denoted as  $T_{cs}$ . We use Born-Oppenheimer (BO) approximation, which treats tetraquarks as color-antitriplet diquark ( $\delta$ ) and antidiquark ( $\bar{\delta}'$ ) pairs connected via a confining flux tube, and allows their spectrum to be calculated in terms of interquark potentials derived from lattice QCD or phenomenological models. Charmed-strange tetraquarks include both a charm and a strange quark, placing them between the fully heavy systems and the more speculative light-flavor tetraquarks. The  $T_{cs}$  states are of particular interest because they offer a unique laboratory where the heavy charm quark provides a static color source, while the strange quark introduces light-flavor dynamics and relativistic effects. This blend allows us to test the limits of the BO approximation and explore whether the same dynamical assumptions valid for heavy tetraquarks can be extended to heavy-light combinations.

This paper is organized as follows: Section II discusses the BO approximation together with dynamical diquark model. In Section III, we present mass spectrum and root-mean-square radius values for  $T_{c\bar{s}0}^a(2900)^0$  and  $T_{c\bar{s}0}^a(2900)^{++}$  states. Section IV is reserved for a summary of this work.

## II. BORN-OPPENHEIMER APPROXIMATION

The BO approximation was developed in the first decade of quantum mechanics [26] and is a tool used in atomic and molecular physics to study how atoms bind together to form molecules. The fundamental concept is to distinguish between the motion of atomic nuclei and electrons so that the large ratio of time scales between their motions can be utilized. It is well known that the mass of the atomic nuclei is considerably large than the mass of the electron. Electrons circle around the atomic nuclei and respond nearly instantaneously to the motion of the atomic nuclei. The atomic nuclei is considerably heavy compared to electron and electrically positive. Atomic nuclei can be thought of as a stationary source of electric field, and their positions determine the configuration of electrons. In this configuration,

the energy of the electrons together with the repulsive Coulomb energy of the atomic nuclei constitutes a BO potential. The final step is to solve the Schrödinger equation using that potential to determine the molecule energy levels [27].

The application of BO approximation to high energy physics systems has similar roots to those of atomic and molecular physics. Systems including heavy quark pairs are laboratories for this application. The BO approximation for heavy quarkonium ( $Q\bar{Q}$ ) states in QCD was developed in Ref. [28]. The application of the BO approximation takes advantage of the large ratio of time scales for the motion of the heavy quark and heavy antiquark as well as the evolution of gluon fields, analogous to in atomic and molecular physics. This is due to the large ratio of the  $m_Q/\Lambda_{\text{QCD}}$ , where  $m_Q$  is the heavy quark mass and  $\Lambda_{\text{QCD}}$  is the energy scale correlated with the gluon field. Similar to how electrons react to the motion of atomic nuclei, the gluon field also responds to the motion of the heavy quark and heavy antiquark, which can be roughly described as a static color field. A BO potential  $V_\Gamma(r)$  is defined by the gluon field energy and depends on the quantum numbers of the gluon field as well as the distance between the heavy quark and heavy antiquark. The energy levels of the Schrödinger equation with the BO potential are known as the heavy quarkonium ( $Q\bar{Q}$ ) states in the BO approximation.

When considering four-quark systems, the BO approximation demands at least two heavy sources and degrees-of-freedom for light quarks. The mass of heavy quark is substantially larger than the mass of light quark,  $m_Q \gg m_q$ . In the presence of heavy color sources, the fast mobility of light quarks generates an effective potential in this limit. Heavy quarks move slowly, which is described by the BO potential [29].

The theoretical description of exotic four-quark states requires distinguishing between two dominant structural pictures: a compact multiquark configuration, where quarks are confined within a single hadronic volume, and a loosely bound hadronic molecule, where hadrons interact via residual nuclear-like forces. A key diagnostic is the system binding energy and spatial extent. For a state near a hadron-hadron threshold, a small binding energy  $B$  leads to a large spatial size, characterized by the root-mean-square radius  $R_{\text{rms}} \sim 1/\sqrt{2\mu B}$ , where  $\mu$  is the reduced mass of the hadron pair. Empirically,  $R_{\text{rms}} > 1$  fm suggests a molecular structure, while  $R_{\text{rms}} < 1$  fm indicates a compact state. This is corroborated by the binding momentum,  $\gamma_b = \sqrt{2\mu B}$ . For canonical hadronic molecules like the  $X(3872)$  [3] and the  $T_{cc}^+$  [30, 31], one finds  $B \lesssim 1$  MeV and thus  $\gamma_b \lesssim 100$  MeV. This molecular binding scale,  $\gamma_b$ , is significantly smaller than the constituent mass of the strange quark,  $m_s^{\text{CQM}} \sim 500$  MeV [32–34]. The hierarchy  $\gamma_b \ll m_s^{\text{CQM}}$  implies that the weak binding forces characteristic of molecules are insufficient to probe the internal structure or excite the internal degrees of freedom of a hadron containing a strange quark. Consequently, in near-threshold dynamics, the strange quark can be treated as an inert, heavy source [21].

This observation provides a foundation for applying the Born-Oppenheimer (BO) approximation to the  $T_{c\bar{s}0}(2900)$  states, which we interpret as a system of a charm-light diquark and a strange-light antidiquark. The BO formalism requires a clear separation of energy scales. The “fast” degrees of freedom are the gluon field and the light ( $u, d$ ) quarks, whose excitation energies for a given source separation are set by the QCD scale,  $\Delta E_{\text{glue/light}} \sim \Lambda_{\text{QCD}} \approx 200 - 300$  MeV, as confirmed by lattice QCD studies of the BO potentials [28, 35]. The “slow” degree of freedom is the relative motion of the heavy diquark and antidiquark.

While the strange quark mass is not as large as the charm mass, its constituent mass satisfies  $m_s^{\text{CQM}} \gtrsim \Lambda_{\text{QCD}}$ . This hierarchy suggests that the strange quark dynamics can be partially decoupled from the faster gluonic and light-quark modes, making the BO approximation a theoretically plausible framework for this system. We note that this treatment introduces systematic uncertainties, particularly for fine structure, estimated to be of order  $\Lambda_{\text{QCD}}/m_s \sim 50 - 100$  MeV. However, for predicting the dominant mass spectrum and structural nature (compact vs. molecular), the approximation is expected to be robust.

The viability of this approach is supported by earlier studies. It has been established that the energies of static-light hadronic systems generate effective BO potentials for heavy multiparton systems [36]. Crucially, the dynamical diquark model has been successfully extended to the hidden-strangeness sector ( $s\bar{s}q\bar{q}$ ), where the BO approximation yielded a viable spectrum of tetraquark states without the presence of a heavier charm or bottom quark [37]. This demonstrates the applicability of the BO formalism to systems where the strange quark acts as the heaviest active flavor. In our case, with both charm and strange quarks present, the justification for the BO approach is further strengthened. The approximation thus allows us to define a confining potential between the diquark and antidiquark based on the response of the gluon and light-quark fields to these heavier color sources.

### A. Dynamical Diquark Model

As already stated, we analyze the spectrum of  $T_{c\bar{s}0}^a(2900)^0$  and  $T_{c\bar{s}0}^a(2900)^{++}$  states within the framework of the dynamical diquark model, leveraging the BO approximation. This approach is rooted in the separation of time scales between the heavy diquark-antidiquark constituents and the more rapidly fluctuating gluonic and light-quark fields. As such, the inter-diquark interaction is modeled by an effective potential derived from the nonperturbative QCD structure connecting the two bodies via a color flux tube. Accordingly, the light degrees of freedom that mediate

the interaction between the static diquark and antidiquark can be described as a function of the separation between the heavy ( $Q\bar{Q}$ ) pair. When the light quark is localized near the heavy quark  $Q$ , the four-quark system effectively assumes the configuration  $(Qq)_{\bar{3}} + (\bar{Q}\bar{q})_3$  where the diquark and antidiquark form a color antitriplet–triplet pair.

We employ dynamical diquark model [38–40] in which exotic states are constructed of heavy-light diquarks  $\delta$  and  $\bar{\delta}$ . These diquarks come into being in attractive channels as  $3 \otimes 3 \rightarrow \bar{3} : [\delta = (Qq)_{\bar{3}}]$  and  $\bar{3} \otimes \bar{3} \rightarrow 3 : [\bar{\delta} = (\bar{Q}\bar{q})_3]$ . The diquark-antidiquark pair in the dynamical diquark model arises instantaneously at the production point and soon separates from one another as a result of the kinematic effects of the production process. Diquark and antidiquark, being colored particles, are unable to split apart; instead, they elongate, forming a color flux tube or string between them. The color flux tube that connects the separated  $\delta - \bar{\delta}$  pair describes its quantized states well in terms of the different potentials that are calculated with the BO approximation. This model was successfully applied to tetraquarks and pentaquarks [41–45].

Ref. [46] focused on the spectroscopy of  $\delta - \bar{\delta}'$  states that do not possess orbital momentum in diquarks, but permit any kind of orbital excitation and gluon-field excitation between diquark pairs. Diquarks are assumed to be pointlike objects and there is no orbital excitation in diquarks. The core states for  $\delta - \bar{\delta}$  systems can be written

$$\begin{aligned} J^{PC} = 0^{++} : \quad & X_0 \equiv |0_\delta, 0_{\bar{\delta}}\rangle_0, \quad X'_0 \equiv |1_\delta, 1_{\bar{\delta}}\rangle_0, \\ J^{PC} = 1^{++} : \quad & X_1 \equiv \frac{1}{\sqrt{2}} (|1_\delta, 0_{\bar{\delta}}\rangle_1 + |0_\delta, 1_{\bar{\delta}}\rangle_1), \\ J^{PC} = 1^{+-} : \quad & Z \equiv \frac{1}{\sqrt{2}} (|1_\delta, 0_{\bar{\delta}}\rangle_1 - |0_\delta, 1_{\bar{\delta}}\rangle_1), \\ & Z' \equiv |1_\delta, 1_{\bar{\delta}}\rangle_1, \\ J^{PC} = 2^{++} : \quad & X_2 \equiv |1_\delta, 1_{\bar{\delta}}\rangle_2 \end{aligned} \quad (7)$$

which is written with the total  $\delta(\bar{\delta})$  spin denoted by  $s_\delta(s_{\bar{\delta}})$ , and the outer subscript gives the overall state total spin. These states specify the full multiplet of  $\Sigma_g^+$   $S$ -wave states.

We construct the  $T_{cs0}$  system as a bound state of a color-antitriplet scalar diquark  $\delta = [cq]_{\bar{3}}$  and an antidiquark  $\bar{\delta}' = [s'q']_3$  where  $q, q' = u, d$ . The product of two color-triplet representations decomposes as  $3 \otimes 3 = \bar{3} \oplus 6$ , and we restrict our study to the attractive antitriplet channel  $\bar{3}$ . The light quark content implies that these states form an isospin triplet  $I = 1$ , for brevity and without loss of generality, we focus on the  $I_3 = \pm 1$  components, though the neutral member can be treated analogously, with only minor mass differences due to electromagnetic corrections.

The quantum numbers of  $T_{cs0}$  states are  $I(J^P) = 1(0)^+$ . They are in the ground state and therefore the multiplet  $\Sigma_g^+(1S)$  are sufficient to accommodate these states. The light quarks inside the  $T_{cs0}$  states have distinct flavor. Therefore isospin quantum number should be taken into account. The isospin effects are studied in detail in Ref. [40]. Here, we follow the same procedure underlying the main features. For further details, see the related reference. The  $S$ -wave Hamiltonian of the model reads as

$$H = H_0 + H_{\kappa_{qQ}} + H_{V_0}. \quad (8)$$

Here  $H_{\kappa_{qQ}}$  is the Hamiltonian for interaction

$$H_{\kappa_{qQ}} = 2\kappa_{qQ}(s_q \cdot s_Q + s_{\bar{q}} \cdot s_{\bar{Q}}) \quad (9)$$

with the  $\kappa_{qQ}$  representing the strength of the spin-spin couplings within diquark and  $H_{V_0}$  is the isopin-interaction term

$$H_{V_0} = V_0 (\tau_q \cdot \tau_{\bar{q}}) (\sigma_q \cdot \sigma_{\bar{q}}) \quad (10)$$

with the  $V_0$  being an isospin operator.

## B. Numerical Aspects

In the dynamical diquark model, the mass spectrum is determined by solving the quantum mechanical problem for the diquark-antidiquark ( $\delta - \bar{\delta}'$ ) pair interacting via a specific Born-Oppenheimer potential,  $V_\Gamma(r)$ . Each potential, labeled by the quantum numbers of the gluon field configuration (e.g.,  $\Sigma_g^+$ ,  $\Sigma_u^+$ ), gives rise to a distinct multiplet of tetraquark states.

The radial wavefunction  $\psi_\Gamma^{(n)}(r)$  and binding energy  $E_n$  for a state with orbital angular momentum  $\ell$  are obtained by solving the corresponding radial Schrödinger equation (in natural units,  $\hbar = c = 1$ ):

$$\left[ -\frac{1}{2\mu r^2} \frac{d}{dr} \left( r^2 \frac{d}{dr} \right) + \frac{\ell(\ell+1)}{2\mu r^2} \right] \psi_\Gamma^{(n)}(r) + V_\Gamma(r) \psi_\Gamma^{(n)}(r) = E_n \psi_\Gamma^{(n)}(r). \quad (11)$$

where  $\mu = m_\delta m_{\bar{\delta}'} / (m_\delta + m_{\bar{\delta}'})$  is the reduced mass of the  $\delta$ - $\bar{\delta}'$  system.

For the central potential  $V_{\Sigma_g^+}(r)$ , we adopt the functional form determined from lattice QCD simulations [35], which accurately captures the non-perturbative confining dynamics. The eigenvalue problem is solved numerically using a finite-difference method on a discretized radial grid, imposing Dirichlet boundary conditions ( $\psi(r) \rightarrow 0$ ). The eigenvalues  $E_n$  are determined via a robust shooting algorithm that matches the logarithmic derivative of the wavefunction, utilizing an adaptive step size for precision.

The computed eigenvalues  $E_n$  represent the binding energies of the  $\delta$ - $\bar{\delta}'$  system. The total mass of the tetraquark state is then given by the sum of the constituent diquark masses and this binding energy:

$$M_{T_{cs}} = m_\delta + m_{\bar{\delta}'} + E_n. \quad (12)$$

### III. NUMERICAL RESULTS

Within the dynamical diquark model, the diquark mass constitutes a fundamental input parameter. To ensure predictions remain independent of specific quark model assumptions, we employ diquark masses obtained through QCD sum rule calculations: for charm-light systems,  $m_{cq} = 1.86 \pm 0.10$  GeV ( $J^P = 0^+$ ) and  $m_{cq} = 1.96 \pm 0.10$  GeV ( $J^P = 1^+$ ) [47]; for strange-light systems,  $m_{sq} = 0.77 \pm 0.04$  GeV ( $J^P = 0^+$ ) and  $m_{sq} = 0.92 \pm 0.04$  GeV ( $J^P = 1^+$ ) [48]. The spin-spin coupling constants  $\kappa_{qq} = 103$  MeV and  $\kappa_{cs} = 25$  MeV are adopted from Ref. [49], while the isospin-dependent interaction strength  $V_0 = 33.10$  MeV follows from hidden-charm tetraquark studies [40]. To assess parameter sensitivity, we consider variations  $V_0 = \{20, 30, 40\}$  MeV, denoted as Sets I, II, and III, respectively.

For the  $T_{c\bar{s}0}^a(2900)$  states with established quantum numbers  $I(J^P) = 1(0^+)$ , the relevant core states are  $X_0$  and  $X'_0$ . While mixing between these configurations is permitted, we deliberately examine pure spin-0 and spin-1 diquark arrangements to isolate their individual contributions to the mass spectrum and spatial structure.

We compute ground-state masses and root-mean-square radii  $\langle r^2 \rangle^{1/2}$ , which characterize the spatial separation within the diquark-antidiquark ( $\delta$ - $\bar{\delta}'$ ) system. Tables II–V present comprehensive numerical results, while Figs. 1–4 provide mass locations between theoretical predictions and experimental measurements.

TABLE II. Mass and root-mean-square radius predictions for  $T_{c\bar{s}0}^a(2900)^0$  with spin-0 diquark configuration  $(cd)(\bar{s}\bar{u})$ . Masses in MeV, radii in fm.

Parameter Set	Mass [MeV]	$\langle r^2 \rangle^{1/2}$ [fm]
Set I	2715	0.70
Set II	2723	0.70
Set III	2730	0.70
Experiment [6, 7]	$2892 \pm 14 \pm 15$	–

TABLE III. Mass and root-mean-square radius predictions for  $T_{c\bar{s}0}^a(2900)^{++}$  with spin-0 diquark configuration. Masses in MeV, radii in fm.

Parameter Set	Mass [MeV]	$\langle r^2 \rangle^{1/2}$ [fm]
Set I	2772	0.72
Set II	2781	0.72
Set III	2792	0.72
Experiment [6, 7]	$2921 \pm 17 \pm 20$	–

A striking pattern emerges from the spin-0 diquark calculations. As evident in Tables II and III, the predicted masses systematically fall approximately 150–160 MeV below experimental values. This substantial and consistent discrepancy across all parameter sets strongly suggests that scalar diquark configurations cannot adequately describe the  $T_{c\bar{s}0}^a(2900)$  states.

In contrast, the spin-1 diquark configurations yield good agreement with experimental data. For  $T_{c\bar{s}0}^a(2900)^0$  (Table IV), the predicted mass range 2881–2894 MeV aligns precisely with the experimental value  $2892 \pm 14 \pm 15$  MeV. Similarly, for  $T_{c\bar{s}0}^a(2900)^{++}$  (Table V), the theoretical range 2940–2950 MeV agrees well with  $2921 \pm 17 \pm 20$  MeV within uncertainties.

TABLE IV. Mass and root-mean-square radius predictions for  $T_{c\bar{s}0}^a(2900)^0$  with spin-1 diquark configuration  $(cd)(\bar{s}\bar{u})$ . Masses in MeV, radii in fm.

Parameter Set	Mass [MeV]	$\langle r^2 \rangle^{1/2}$ [fm]
Set I	2881	0.77
Set II	2886	0.77
Set III	2894	0.77
Experiment [6, 7]	$2892 \pm 14 \pm 15$	–

TABLE V. Mass and root-mean-square radius predictions for  $T_{c\bar{s}0}^a(2900)^{++}$  with spin-1 diquark configuration. Masses in MeV, radii in fm.

Parameter Set	Mass [MeV]	$\langle r^2 \rangle^{1/2}$ [fm]
Set I	2940	0.80
Set II	2944	0.80
Set III	2950	0.80
Experiment [6, 7]	$2921 \pm 17 \pm 20$	–

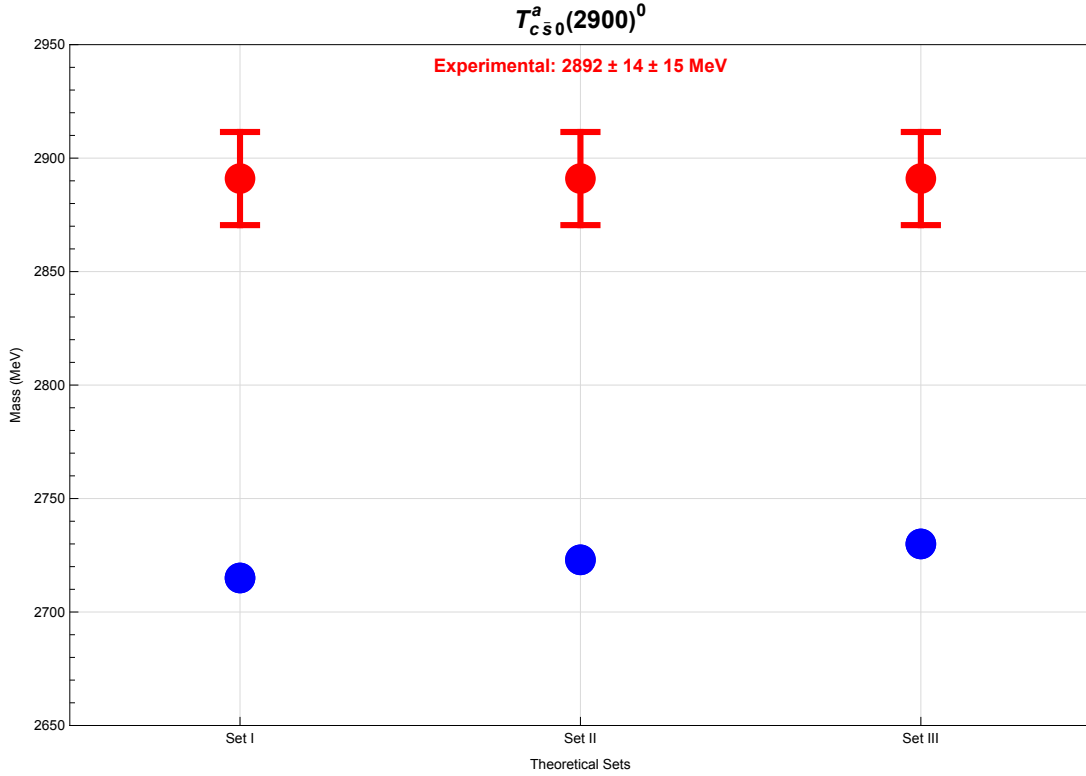


FIG. 1. Mass predictions for  $T_{c\bar{s}0}^a(2900)^0$  with spin-0 diquark configuration compared to experimental data.

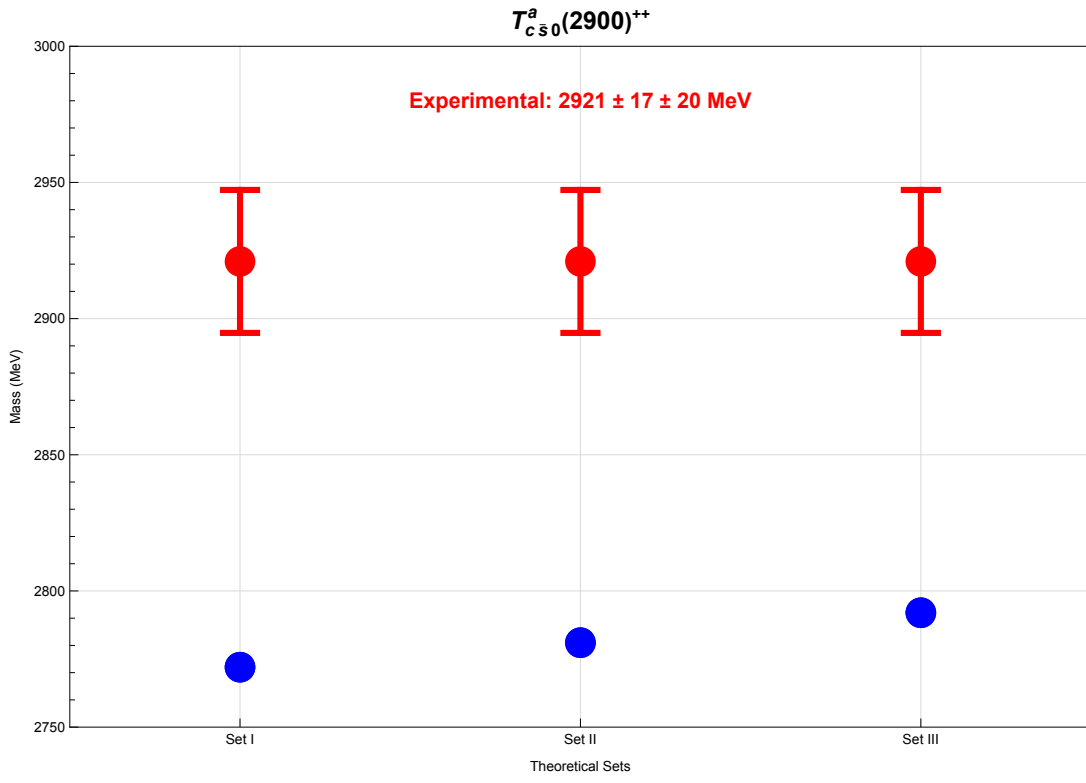


FIG. 2. Mass predictions for  $T_{c\bar{s}0}^a(2900)^{++}$  with spin-0 diquark configuration compared to experimental data.

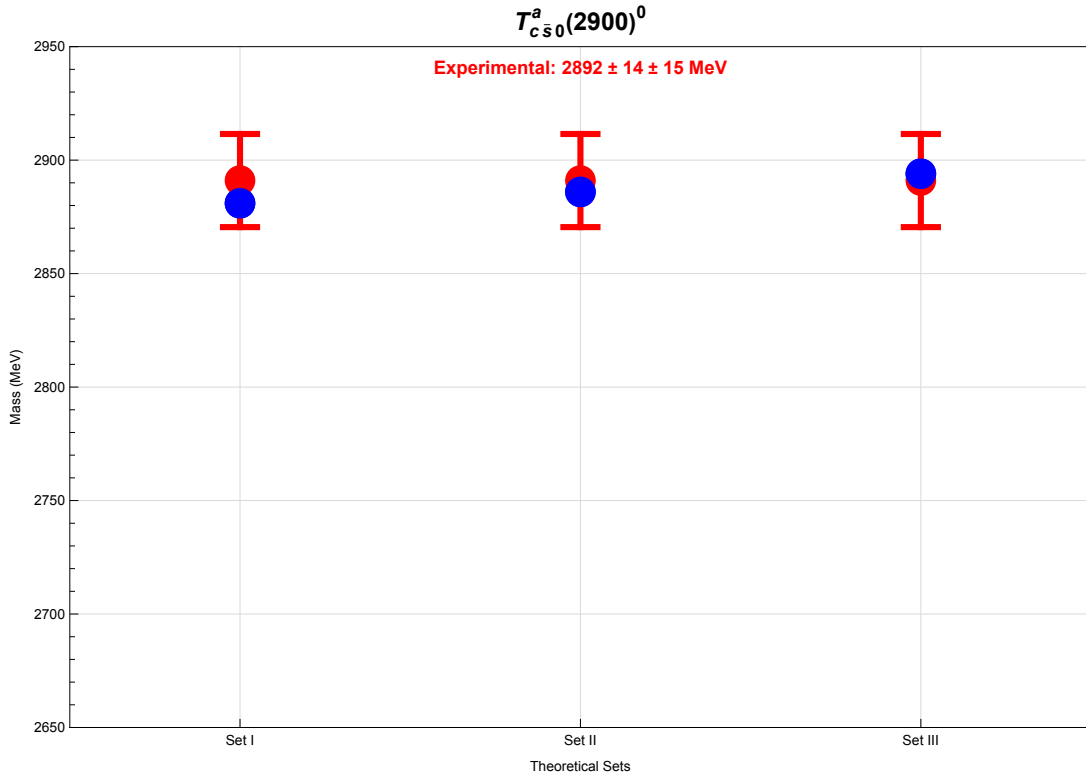


FIG. 3. Mass predictions for  $T_{c\bar{s}0}^a(2900)^0$  with spin-1 diquark configuration compared to experimental data.



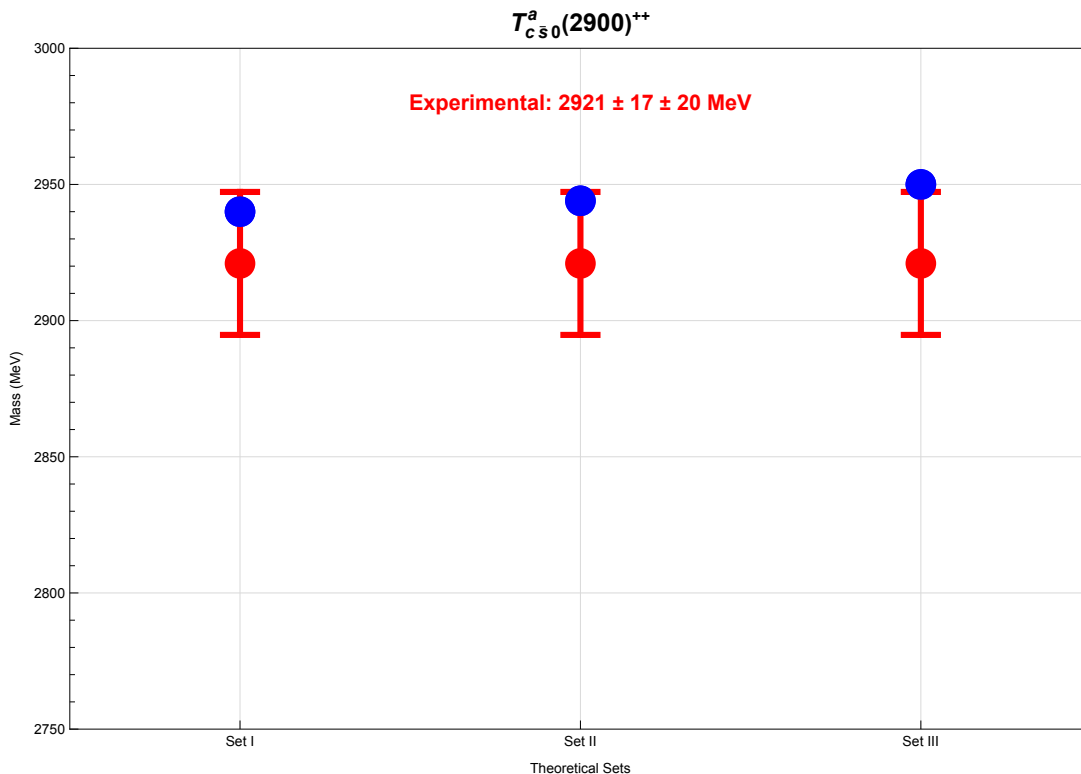


FIG. 4. Mass predictions for  $T_{c\bar{s}0}^a(2900)^{++}$  with spin-1 diquark configuration compared to experimental data.

The locations of predicted masses in Figs. 1–4 reinforce these conclusions, clearly demonstrating the systematic failure of spin-0 configurations and the remarkable success of spin-1 arrangements in reproducing experimental masses. The mass splitting between neutral and charged states exhibits remarkable consistency across configurations:  $\Delta M = 57\text{--}62$  MeV for spin-0 and  $56\text{--}59$  MeV for spin-1 diquarks. This robust pattern, maintained throughout our parameter variations, aligns well with experimental observations and reflects the isospin triplet nature of these states. The theoretical predictions display minimal sensitivity to the isospin parameter  $V_0$ , with mass variations of only  $\sim 13$  MeV across Sets I–III. The  $V_0$ -induced shifts remain below 20 MeV, indicating that while isospin effects contribute to mass splittings, they play a subdominant role in overall mass generation.

The calculated root-mean-square radii,  $\langle r^2 \rangle^{1/2} = 0.70\text{--}0.80$  fm, indicate that the  $T_{c\bar{s}}(2900)$  states are spatially compact, lying well below the characteristic hadronic scale of 1 fm. Such compactness strongly disfavors loosely bound molecular interpretations and instead supports a genuine tetraquark configuration. This behavior aligns naturally with expectations from color flux tube dynamics and is consistent with previous analyses of similarly structured multiquark systems [14].

The successful mass reproduction with spin-1 diquarks implies specific structural assignments:  $T_{c\bar{s}0}^a(2900)^0$  as  $[cd]_{\frac{1}{2}^+}^+ \otimes [\bar{s}u]_{\frac{1}{2}^+}^+$  and  $T_{c\bar{s}0}^a(2900)^{++}$  as  $[cu]_{\frac{1}{2}^+}^+ \otimes [\bar{s}d]_{\frac{1}{2}^+}^+$ . These axial-vector diquark configurations naturally accommodate the established quantum numbers  $I(J^P) = 1(0^+)$  while accurately reproducing the observed mass spectrum.

The good agreement between theoretical predictions and experimental data for spin-1 diquark configurations validates several key theoretical elements. First, the BO approximation demonstrates effectiveness for mixed heavy-light systems, with the strange quark serving as an adequate static source in near-threshold dynamics. Second, the dynamical diquark model demonstrates consistent predictive capability in the open-charm sector as well, complementing its established applications to fully heavy tetraquarks [44, 50].

#### IV. CONCLUSION

In this work, we have analyzed the open-charm tetraquark candidates  $T_{c\bar{s}0}^a(2900)^0$  and  $T_{c\bar{s}0}^a(2900)^{++}$  within the dynamical diquark model supplemented by the BO approximation. The near-threshold production of these states suggests that the strange quark is not strongly perturbed by short-range dynamics inside the tetraquark, permitting its treatment as an effectively heavy, or quasi-heavy, degree of freedom. This motivates the application of BO methods,



in which the diquark–antidiquark motion evolves in a confining potential derived from lattice QCD.

Our analysis clearly demonstrates that the internal spin structure of the diquark plays a decisive role in determining the spectroscopy of the  $T_{c\bar{s}0}^a(2900)$  multiplet. When the constituent clusters are modeled as scalar ( $J^P = 0^+$ ) diquarks, the predicted masses undershoot the experimental values by approximately 150–160 MeV for both charge states. Such a persistent and parameter-stable deficit—substantially larger than any plausible theoretical uncertainty in the diquark masses or in the BO potential—rules out scalar diquarks as the dominant component of the observed resonances.

In contrast, the axial-vector ( $J^P = 1^+$ ) diquark configuration successfully reproduces the experimental spectrum. The predicted ranges 2881–2894 MeV for  $T_{c\bar{s}0}^a(2900)^0$  and 2940–2950 MeV for  $T_{c\bar{s}0}^a(2900)^{++}$  closely match the LHCb values once uncertainties are taken into account. The fact that a single underlying configuration  $[cq]_{1+}[\bar{s}\bar{q}]_{1+}$  describes both charge states without tuning strongly supports the interpretation of these resonances as compact axial-vector tetraquarks.

The preference for the axial-vector configuration can also be understood through the effective heavy-quark behavior of the strange quark and the structure of lattice BO potentials. In the near-threshold regime relevant for  $T_{c\bar{s}}$  states, the strange quark is not significantly excited by the long-range dynamics of the tetraquark and thus behaves as a quasi-heavy degree of freedom. This suppresses spin-sensitive transitions in the  $\bar{s}\bar{q}$  antidiquark and enhances the stability of the axial-vector  $[cq]_{1+}$  configuration, whose internal hyperfine structure is more robust against the reduced light-quark spin interactions. Furthermore, the lattice-determined  $\Sigma_g^+$  BO potential exhibits a confining structure consistent with a heavy static color source interacting with a lighter partner, a pattern naturally compatible with the intermediate mass scale of the strange quark. The combined effect of quasi-heavy strange-quark dynamics, reduced spin excitations, and the confining BO potential therefore provides a unified explanation for why only the axial-vector diquark configuration reproduces the observed  $T_{c\bar{s}0}^a(2900)$  spectrum.

The predicted isospin mass splitting,  $\Delta M = M^{++} - M^0 \simeq 56\text{--}62$  MeV, is stable across all parameter sets, indicating that the splitting arises primarily from the flavor and color–spin structure of the diquark–antidiquark system. This magnitude is consistent with expectations from  $u$ – $d$  mass differences and earlier studies of isovector heavy–light tetraquarks.

The spatial information extracted from the BO wavefunctions further confirms the compact nature of these states. The rms radii of both charge states lie within 0.70–0.80 fm, well below the molecular scale  $\gtrsim 1$  fm, decisively disfavoring extended  $D^{(*)}K^{(*)}$  configurations. These radii are instead compatible with short-range confinement and the formation of a color flux tube between the diquark and antidiquark.

Taken together, the mass spectrum, isospin structure, and spatial properties paint a coherent and unified picture: the  $T_{c\bar{s}0}^a(2900)$  resonances are best interpreted as compact diquark–antidiquark tetraquarks dominated by axial-vector diquark components. The dynamical diquark model, augmented with BO dynamics, therefore provides a predictive and internally consistent framework for describing open-flavor exotics and reveals structural patterns that may extend to bottom–charm, charm–strange, and other mixed heavy–light tetraquark systems.

Further theoretical developments—including spin-dependent splittings, BO-channel mixing, and decay-width calculations—will refine this picture. Experimentally, improved Dalitz analyses of  $B^0 \rightarrow \bar{D}^0 D_s^+ \pi^-$  and  $B^+ \rightarrow D^- D_s^+ \pi^+$ , as well as searches for additional isospin partners, will be essential for fully establishing the internal dynamics and flavor structure of these intriguing states.

- 
- [1] M. Gell-Mann, A Schematic Model of Baryons and Mesons, Phys. Lett. 8 (1964) 214–215. [doi:10.1016/S0031-9163\(64\)92001-3](https://doi.org/10.1016/S0031-9163(64)92001-3).
  - [2] G. Zweig, Developments in the quark theory of hadrons, CERN Report No.8182/TH.401, CERN Report No.8419/TH.412 (1964).
  - [3] S. K. Choi, et al., Observation of a narrow charmonium-like state in exclusive  $B^\pm \rightarrow K^\pm \pi^+ \pi^- J/\psi$  decays, Phys. Rev. Lett. 91 (2003) 262001. [arXiv:hep-ex/0309032](https://arxiv.org/abs/hep-ex/0309032), [doi:10.1103/PhysRevLett.91.262001](https://doi.org/10.1103/PhysRevLett.91.262001).
  - [4] R. Aaij, et al., Amplitude analysis of the  $B^+ \rightarrow D^+ D^- K^+$  decay, Phys. Rev. D 102 (2020) 112003. [arXiv:2009.00026](https://arxiv.org/abs/2009.00026), [doi:10.1103/PhysRevD.102.112003](https://doi.org/10.1103/PhysRevD.102.112003).
  - [5] R. Aaij, et al., A model-independent study of resonant structure in  $B^+ \rightarrow D^+ D^- K^+$  decays, Phys. Rev. Lett. 125 (2020) 242001. [arXiv:2009.00025](https://arxiv.org/abs/2009.00025), [doi:10.1103/PhysRevLett.125.242001](https://doi.org/10.1103/PhysRevLett.125.242001).
  - [6] R. Aaij, et al., Amplitude analysis of  $B^0 \rightarrow D^- D_s^+ \pi^-$  and  $B^+ \rightarrow D^- D_s^+ \pi^+$  decays, Phys. Rev. D 108 (1) (2023) 012017. [arXiv:2212.02717](https://arxiv.org/abs/2212.02717), [doi:10.1103/PhysRevD.108.012017](https://doi.org/10.1103/PhysRevD.108.012017).
  - [7] R. Aaij, et al., First Observation of a Doubly Charged Tetraquark and Its Neutral Partner, Phys. Rev. Lett. 131 (4) (2023) 041902. [arXiv:2212.02716](https://arxiv.org/abs/2212.02716), [doi:10.1103/PhysRevLett.131.041902](https://doi.org/10.1103/PhysRevLett.131.041902).
  - [8] R. Chen, Q. Huang, From the isovector molecular explanation of the newly  $T_{c\bar{s}}^{a0(++)}(2900)$  to possible charmed-strange molecular pentaquarks (8 2022). [arXiv:2208.10196](https://arxiv.org/abs/2208.10196).
  - [9] S. S. Agaev, K. Azizi, H. Sundu, Modeling the resonance  $T_{cs0a}(2900)^{++}$  as a hadronic molecule  $D^*+K^*$ , Phys. Rev. D 107 (9) (2023) 094019. [arXiv:2212.12001](https://arxiv.org/abs/2212.12001), [doi:10.1103/PhysRevD.107.094019](https://doi.org/10.1103/PhysRevD.107.094019).

- [10] Z.-L. Yue, C.-J. Xiao, D.-Y. Chen, Decays of the fully open flavor state  $T_{cs}^{-00}$  in a  $D^*K^*$  molecule scenario, Phys. Rev. D 107 (3) (2023) 034018. [arXiv:2212.03018](#), [doi:10.1103/PhysRevD.107.034018](#).
- [11] F.-X. Liu, R.-H. Ni, X.-H. Zhong, Q. Zhao, Charmed-strange tetraquarks and their decays in the potential quark model, Phys. Rev. D 107 (9) (2023) 096020. [arXiv:2211.01711](#), [doi:10.1103/PhysRevD.107.096020](#).
- [12] X.-S. Yang, Q. Xin, Z.-G. Wang, Analysis of the  $T_{cs}(2900)$  and related tetraquark states with the QCD sum rules, Int. J. Mod. Phys. A 38 (11) (2023) 2350056. [arXiv:2302.01718](#), [doi:10.1142/S0217751X23500562](#).
- [13] D.-K. Lian, W. Chen, H.-X. Chen, L.-Y. Dai, T. G. Steele, Strong decays of  $T_{cs0}^a(2900)^{++/0}$  as a fully open-flavor tetraquark state, Eur. Phys. J. C 84 (1) (2024) 1. [arXiv:2302.01167](#), [doi:10.1140/epjc/s10052-023-12355-4](#).
- [14] J. Wei, Y.-H. Wang, C.-S. An, C.-R. Deng, Color flux-tube nature of the states  $T_{cs}(2900)$  and  $T_{cs}^{-a}(2900)$ , Phys. Rev. D 106 (9) (2022) 096023. [arXiv:2210.04841](#), [doi:10.1103/PhysRevD.106.096023](#).
- [15] P. G. Ortega, D. R. Entem, F. Fernandez, J. Segovia, Novel  $T_{cs}$  and  $T_{cs}^{-}$  candidates in a constituent-quark-model-based meson-meson coupled-channels calculation, Phys. Rev. D 108 (9) (2023) 094035. [arXiv:2305.14430](#), [doi:10.1103/PhysRevD.108.094035](#).
- [16] H.-W. Ke, Y.-F. Shi, X.-H. Liu, X.-Q. Li, Possible molecular states of  $D^{-*}K^*$  ( $D^*K^*$ ) and new exotic states  $X0(2900)$ ,  $X1(2900)$ ,  $T_{cs0a}(2900)0$  and  $T_{cs0a}(2900)++$ , Phys. Rev. D 106 (11) (2022) 114032. [arXiv:2210.06215](#), [doi:10.1103/PhysRevD.106.114032](#).
- [17] S. S. Agaev, K. Azizi, H. Sundu, On the structures of new scalar resonances  $T_{cs0}^a(2900)^{++}$  and  $T_{cs0}^a(2900)^0$ , J. Phys. G 50 (5) (2023) 055002. [arXiv:2207.02648](#), [doi:10.1088/1361-6471/acc41a](#).
- [18] R. Molina, E. Oset,  $T_{cs}^{-}(2900)$  as a threshold effect from the interaction of the  $D^*K^*$ ,  $D_s^*\rho$  channels, Phys. Rev. D 107 (5) (2023) 056015. [arXiv:2211.01302](#), [doi:10.1103/PhysRevD.107.056015](#).
- [19] M.-Y. Duan, M.-L. Du, Z.-H. Guo, E. Wang, D.-Y. Chen, Coupled-channel  $D^*K^* - D_s^*\rho$  interactions and the origin of  $T_{cs0}(2900)$ , Phys. Rev. D 108 (7) (2023) 074006. [arXiv:2307.04092](#), [doi:10.1103/PhysRevD.108.074006](#).
- [20] M.-Y. Duan, E. Wang, D.-Y. Chen, Searching for the open flavor tetraquark  $T_{cs0}(2900)^{++}$  in the process  $B^+ \rightarrow K^+ D^+ D^-$ , Eur. Phys. J. C 84 (7) (2024) 681. [arXiv:2305.09436](#), [doi:10.1140/epjc/s10052-024-13044-6](#).
- [21] B. Wang, K. Chen, L. Meng, S.-L. Zhu, Spectrum of the molecular tetraquarks: Unraveling the  $T_{cs0}(2900)$  and  $T_{cs}^{-0a}(2900)$ , Phys. Rev. D 109 (3) (2024) 034027. [arXiv:2309.02191](#), [doi:10.1103/PhysRevD.109.034027](#).
- [22] W.-T. Lyu, Y.-H. Lyu, M.-Y. Duan, D.-M. Li, D.-Y. Chen, E. Wang, Roles of the  $T_{cs}^{-0}(2900)0$  and  $D0^*(2300)$  in the process  $B \rightarrow Ds + K + \pi^-$ , Phys. Rev. D 109 (1) (2024) 014008. [arXiv:2306.16101](#), [doi:10.1103/PhysRevD.109.014008](#).
- [23] M. C. Gordillo, J. Segovia, Diffusion Monte Carlo calculation of compact  $T_{cs0}$  and  $T_{cs}^{-0}$  tetraquarks, Phys. Lett. B 870 (2025) 139927. [arXiv:2507.10346](#), [doi:10.1016/j.physletb.2025.139927](#).
- [24] Z. Yu, Q. Wu, Z.-L. Yue, D.-Y. Chen,  $T_{cs1}^0$  production in the  $B^+$  decays processes (11 2025). [arXiv:2511.18072](#).
- [25] R. Aaij, et al., Observation of New Charmonium or Charmoniumlike States in  $B \rightarrow D^*\pm D \mp K^+$  Decays, Phys. Rev. Lett. 133 (13) (2024) 131902. [arXiv:2406.03156](#), [doi:10.1103/PhysRevLett.133.131902](#).
- [26] M. Born, R. Oppenheimer, Zur Quantentheorie der Molekeln, Annalen Phys. 389 (20) (1927) 457–484. [doi:10.1002/andp.19273892002](#).
- [27] E. Braaten, C. Langmack, D. H. Smith, Born-Oppenheimer Approximation for the XYZ Mesons, Phys. Rev. D 90 (1) (2014) 014044. [arXiv:1402.0438](#), [doi:10.1103/PhysRevD.90.014044](#).
- [28] K. J. Juge, J. Kuti, C. J. Morningstar, Ab initio study of hybrid anti-b g b mesons, Phys. Rev. Lett. 82 (1999) 4400–4403. [arXiv:hep-ph/9902336](#), [doi:10.1103/PhysRevLett.82.4400](#).
- [29] L. Maiani, A. Pilloni, A. D. Polosa, V. Riquer, Doubly heavy tetraquarks in the Born-Oppenheimer approximation, Phys. Lett. B 836 (2023) 137624. [arXiv:2208.02730](#), [doi:10.1016/j.physletb.2022.137624](#).
- [30] R. Aaij, et al., Observation of an exotic narrow doubly charmed tetraquark, Nature Phys. 18 (7) (2022) 751–754. [arXiv:2109.01038](#), [doi:10.1038/s41567-022-01614-y](#).
- [31] R. Aaij, et al., Study of the doubly charmed tetraquark  $T_{cc}^+$ , Nature Commun. 13 (1) (2022) 3351. [arXiv:2109.01056](#), [doi:10.1038/s41467-022-30206-w](#).
- [32] R.-H. Ni, Q. Li, X.-H. Zhong, Mass spectra and strong decays of charmed and charmed-strange mesons, Phys. Rev. D 105 (5) (2022) 056006. [arXiv:2110.05024](#), [doi:10.1103/PhysRevD.105.056006](#).
- [33] R. Chen, Q. Huang, Possible open charm molecular pentaquarks from  $\Lambda_c K^*/\Sigma_c K^*$  interactions, Phys. Rev. D 108 (5) (2023) 054011. [arXiv:2307.04168](#), [doi:10.1103/PhysRevD.108.054011](#).
- [34] B. Silvestre-Brac, Spectrum and static properties of heavy baryons, Few Body Syst. 20 (1996) 1–25. [doi:10.1007/s006010050028](#).
- [35] K. J. Juge, J. Kuti, C. Morningstar, Fine structure of the QCD string spectrum, Phys. Rev. Lett. 90 (2003) 161601. [arXiv:hep-lat/0207004](#), [doi:10.1103/PhysRevLett.90.161601](#).
- [36] E. Braaten, How the  $Z_c(3900)$  Reveals the Spectra of Quarkonium Hybrid and Tetraquark Mesons, Phys. Rev. Lett. 111 (2013) 162003. [arXiv:1305.6905](#), [doi:10.1103/PhysRevLett.111.162003](#).
- [37] S. Jafarzade, R. F. Lebed, Hidden-strangeness tetraquarks in the dynamical diquark model, Phys. Rev. D 112 (1) (2025) 014034. [arXiv:2505.15704](#), [doi:10.1103/4t78-3tc3](#).
- [38] S. J. Brodsky, D. S. Hwang, R. F. Lebed, Dynamical Picture for the Formation and Decay of the Exotic XYZ Mesons, Phys. Rev. Lett. 113 (11) (2014) 112001. [arXiv:1406.7281](#), [doi:10.1103/PhysRevLett.113.112001](#).
- [39] J. F. Giron, R. F. Lebed, C. T. Peterson, The Dynamical Diquark Model: First Numerical Results, JHEP 05 (2019) 061. [arXiv:1903.04551](#), [doi:10.1007/JHEP05\(2019\)061](#).
- [40] J. F. Giron, R. F. Lebed, C. T. Peterson, The Dynamical Diquark Model: Fine Structure and Isospin, JHEP 01 (2020) 124. [arXiv:1907.08546](#), [doi:10.1007/JHEP01\(2020\)124](#).

- [41] J. F. Giron, R. F. Lebed, Spectrum of  $p$ -wave hidden-charm exotic mesons in the diquark model, Phys. Rev. D 101 (7) (2020) 074032. [arXiv:2003.02802](#), [doi:10.1103/PhysRevD.101.074032](#).
- [42] J. F. Giron, R. F. Lebed, Spectrum of the hidden-bottom and the hidden-charm-strange exotics in the dynamical diquark model, Phys. Rev. D 102 (1) (2020) 014036. [arXiv:2005.07100](#), [doi:10.1103/PhysRevD.102.014036](#).
- [43] J. F. Giron, R. F. Lebed, S. R. Martinez, Spectrum of hidden-charm, open-strange exotics in the dynamical diquark model, Phys. Rev. D 104 (5) (2021) 054001. [arXiv:2106.05883](#), [doi:10.1103/PhysRevD.104.054001](#).
- [44] H. Mutuk, Spectrum of  $ccb^-b^-$ ,  $bcc^-c^-$ , and  $bc b^-b^-$  tetraquark states in the dynamical diquark model, Phys. Lett. B 834 (2022) 137404. [arXiv:2208.11048](#), [doi:10.1016/j.physletb.2022.137404](#).
- [45] R. F. Lebed, S. R. Martinez, Exotic hadrons from scattering in the diabatic dynamical diquark model, Phys. Rev. D 108 (1) (2023) 014013. [arXiv:2305.09146](#), [doi:10.1103/PhysRevD.108.014013](#).
- [46] R. F. Lebed, Spectroscopy of Exotic Hadrons Formed from Dynamical Diquarks, Phys. Rev. D 96 (11) (2017) 116003. [arXiv:1709.06097](#), [doi:10.1103/PhysRevD.96.116003](#).
- [47] Z.-G. Wang, Analysis of the scalar and axial-vector heavy diquark states with QCD sum rules, Eur. Phys. J. C 71 (2011) 1524. [arXiv:1008.4449](#), [doi:10.1140/epjc/s10052-010-1524-y](#).
- [48] Z.-G. Wang, Analysis of the light-flavor scalar and axial-vector diquark states with QCD sum rules, Commun. Theor. Phys. 59 (2013) 451–456. [arXiv:1112.5910](#), [doi:10.1088/0253-6102/59/4/11](#).
- [49] L. Maiani, F. Piccinini, A. D. Polosa, V. Riquer, Diquark-antidiquarks with hidden or open charm and the nature of  $X(3872)$ , Phys. Rev. D 71 (2005) 014028. [arXiv:hep-ph/0412098](#), [doi:10.1103/PhysRevD.71.014028](#).
- [50] J. F. Giron, R. F. Lebed, Simple spectrum of  $c\bar{c}c\bar{c}$  states in the dynamical diquark model, Phys. Rev. D 102 (7) (2020) 074003. [arXiv:2008.01631](#), [doi:10.1103/PhysRevD.102.074003](#).